Mechanical properties of precipitation strengthening Cu-base alloys highly deformed by ARB process

ICM11

Mechanical Properties of Precipitation Strengthening Cu-Base Alloys Highly Deformed by ARB Process

R. Monzen[a*], Y. Takagawa[a], C Watanabe[a], D. Terada[b] and N. Tsuji[b]

[a]*Division of Innovative Technology and Science, Kanazawa University, Kanazawa 920-1192, Japan*
[b]Department of Materials Science and Engineering, Kyoto University, Yoshida Honmachi, Sakyo-ku, Kyoto 606-8501, Japan

Abstract

The enhancement of strength of Cu-1.2wt%Ni-0.2wt%Be-0.1wt%Zr and Cu-1.4wt%Ni-0.25wt%P-0.1wt%Zr alloys has been tried by the combination of ARB process by 5 cycles and aging treatment at 350 to 450°C. The grain sizes of the alloys, severely deformed by 5-cycle ARB process, were refined down to about 0.4μm. The Cu-Ni-Be-Zr alloy, ARB-processed and peak-aged at 375°C, exhibited a tensile strength σ_u of 810MPa, an elongation ε_t of 9% up to failure and an electrical conductivity σ of 62%IACS. The Cu-Ni-P-Zr alloy, initially aged at 450°C, then ARB-processed and peak-aged at 400°C, had the values of σ_u=780MPa, ε_t =6% and σ=56%IACS.

keywords: Cu-Ni-Be alloy; Cu-Ni-P alloy; ARB process; tensile property; grain refinement strengthening; precipitation strengthening; dislocation strengthening

1. Introduction

Cu-base alloys are used for electrical parts such as connectors and lead frames because the electrical conductivity of the alloys is very high. The high strength of the Cu-base alloys is also required for small devices used in microelectronics. Most of the alloys are usually of the precipitation-strengthened types and are dilutely alloyed with elements of very low solubility to preserve high levels of conductivity. Cu-Be alloys are one of the precipitation-hardenable Cu-base alloys, and are used as metallic materials with high strength and conductivity. However, since Be is toxic and expensive, it is required that advanced metallic materials are developed as an alternative to Cu-Be alloys or the amount of Be is lowered.

Recently, a Cu-1.27wt%Ni-0.22wt%Be alloy, which contains smaller amounts of Ni and Be than standard Cu-Ni-Be alloys, has been developed. The strength and electrical conductivity of the Cu-Ni-Be alloy and a standard Cu-2.05wt%Ni-0.35wt%Be alloy aged at 360 to 500°C after cold rolling have been examined [1]. The former alloy exhibits a lower strength and a higher electrical conductivity than the latter alloy. Both alloys are hardened by disk-shaped coherent precipitates of γ” phase. Cu-Ni-P alloys, containing about 0.7wt%Ni and 0.14wt%P, is also one of the typical Cu-base precipitation hardening type alloys [2]. The alloys have high electrical conductivity, but low strength.

In this study, we have tried to enhance the strength of a Cu-1.2wt%Ni-0.2wt%Be-0.1wt%Zr alloy and a Cu-1.4wt%Ni-0.25wt%P-0.1wt%Zr alloy, in which the Ni and P contents are about twice larger than those in commercial Cu-Ni-P alloys, by means of combining accumulative roll-bonding (ARB) process by 5 cycles and aging treatment at 350 to 450ºC. For the sake of comparison, the mechanical properties of the alloys conventionally cold-rolled to a reduction of 50% and 90% and aged at 350 to 450ºC have also been studied. Watanabe *et al.* [3] have

* Corresponding author. Tel.: +81-76-234-4678; fax: +81-76-264-6495.
E-mail address: monzen@t.kanazawa-u.ac.jp.

reported that the addition of small amounts of Zr to Cu-Ni-Si alloys suppresses recrystallization of the alloys highly deformed. This is the reason why 0.1%Zr is added.

2. Experimental

Cu-1.2%Ni-0.2%Be-0.1%Zr and Cu-1.4%Ni-0.25%P-0.1%Zr alloys were prepared by melting in an Argon atmosphere. Rolled sheets of the former and latter alloys were solutionized at 1000ºC for 4 h and 850ºC for 1 h in a vacuum and then water quenched. The average grain sizes for the former and latter alloys after the solution treatments were about 40 and 50 μm, respectively. The solution-treated Cu-Ni-Be-Zr and Cu-Ni-P-Zr sheets were un-aged or aged at 450ºC for 5min, cold-rolled to a 50% and 90% reduction and then aged at 350 to 450ºC. The Cu-Ni-Be-Zr and Cu-Ni-P-Zr sheets solutionized or the Cu-Ni-P-Zr sheets, solutionized and then pre-aged at 450ºC for 5min, were used as the starting sheets for the ARB process. The principle and detailed processing procedures of the ARB process have been reported previously [4]. The ARB process using 50% reduction per cycle was carried out by 5 ARB cycles (equivalent strain = 4.0) with lubrication at room temperature. Then the ARB-processed Cu-Ni-Be-Zr and Cu-Ni-P-Zr sheets were aged at 350 to 450ºC.

Microhardness tests were carried out using the Vickers method. Electrical resistivity measurements were made by a Hocking AutoSigma 3000 electrical conductivity tester at 20ºC.

The microstructural characterization of the specimens was carried out by electron backscattering diffraction (EBSD) pattern measurement and transmission electron microscopy (TEM). The EBSD measurements were carried out in a field emission type scanning electron microscope equipped with a TSL-OIM system at an accelerating voltage of 15 kV. The step size used in the EBSD measurements was 0.05μm. Thin foils for TEM observations were prepared using a twin-jet polishing method with a solution of 80% methanol and 20% nitric acid at -35ºC and 7V. TEM was performed using a JEOL 2010FEF and a Hitachi H-9000NAR microscope at operating voltages of 200kV and 300kV, respectively.

Dislocation density in each specimen was estimated by the Warren-Aberbach method based on the Williamson-Hall plot using the conventional X-ray diffraction data of (111), (200), (220) and (311) reflections. The detailed explanation has been given elsewhere [5].

3. Results

Figures 1(a) and (b) show grain boundary maps obtained from the EBSD measurements of the Cu-Ni-Be-Zr alloy specimens, ARB-processed by 5 cycles and cold-rolled to a 90% reduction. Solid lines indicate high-angle boundaries with a misorientation larger than 15º, while dotted lines are low-angle boundaries with misorientations ranging from 2º to 15º.The boundaries with a misorientation smaller than 2º were cut off, in order to remove this inaccuracy from the EBSD measurement and analysis. The EBSD measurement revealed that the grain sizes of the Cu-Ni-Be-Zr and Cu-Ni-P-Zr alloys, severely deformed by the 5-cycle ARB process or 90% cold-rolling, were nearly identical and refined down to about 0.4 or 4μm. The grain size is defined as the mean spacing of boundaries along the direction normal to the rolling

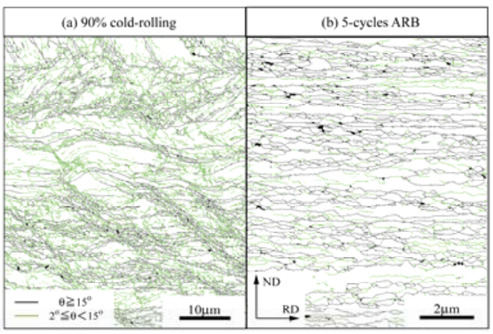

Fig. 1 EBSD boundary maps of the Cu-1.2wt%Ni-0.2wt%Be-0.1wt%Zr specimens, (a) cold-rolled to a 90% reduction and (b) ARB-processed by 5 cycles. In the boundary maps, dotted lines represent the low-angle boundaries having misorientation θ of 2º<θ<15º, while solid lines indicate the high-angle boundaries with θ>15º.

direction. The 90%-rolled specimen showed a typical deformation microstructure where initial grains involving substructures were elongated in the rolling direction (RD). After 5-cycle ARB, the ultrafine lamellar boundary structure was found.

The hardness changes of the solution-treated Cu-Ni-Be-Zr and Cu-Ni-P-Zr alloys after 50% and 90% cold-rolling and ARB process were examined during aging at 350 to 450ºC. For the 50%-rolled Cu-Ni-Be-Zr and Cu-Ni-P-Zr alloys, the peak hardness effect occurred when aged at 450ºC for 2 h and 1 h, respectively. The hardness for the Cu-Ni-Be-Zr alloy, 90%-rolled or ARB-processed and then aged at 375ºC, attained a peak at 10 h and then decreased, and recrystallization was observed after aging for about 14 h. For the Cu-Ni-P-Zr alloy, 90%-rolled or ARB-processed and then aged at 350ºC, the hardness reached a maximum at 30min, at which recrystallization started to occur. As the recrystallization proceeded, the hardness decreased.

Table 1 summarizes the grain size d, 0.2% proof stress $\sigma_{0.2}$, ultimate tensile strength σ_u, elongation ε_t and electrical conductivity σ for the Cu-Ni-Be-Zr specimens, peak-aged at 450ºC for 2 h after 50% cold-rolling, and at 375ºC for 10 h after 90% cold-rolling and ARB process. In order of the 50%-rolled, 90%-rolled and ARB-processed specimens, the strength increases. The value of σ for the 50%-rolled specimens (50%-RS) is smaller than those for the 90%-rolled specimen (90%-RS) and ARB-processed specimen (ARB-PS), which are nearly identical. It should be noted that the Cu-Ni-Be-Zr alloy, ARB-processed and then peak-aged at 375ºC, exhibits the values of σ_u=810MPa, ε_t=9% and σ=62%IACS. The values of σ_u and σ for the ARB-processed and aged specimen is comparable to those for a commercial Cu-1.8%Ni-0.4%Be alloy, σ_u=810MPa and σ =63%IACS [1]. However, the value of ε_t=9% is smaller than the value of ε_t=13% for the commercial alloy.

In Table 1, the values of d, $\sigma_{0.2}$, σ_u, ε_t and σ for the Cu-Ni-P-Zr specimens, peak-aged at 450ºC for 1 h after 50% rolling, and aged at 350ºC for 30min after 90% rolling and ARB process, also are listed. The values of σ_u=640MPa and σ=42%IACS for the ARB-PS are smaller than those of σ_u=670MPa and σ=65%IACS for a commercial Cu-0.7%Ni-0.13%P-0.1%Fe alloy, recently developed [6]. It should be

Table 1 Grain size d, 0.2% proof stress $\sigma_{0.2}$, tensile strength σ_u, elongation ε_t and electrical conductivity σ for the Cu-Ni-Be-Zr specimens, peak-aged (AG) at 450°C for 2 h after 50% cold-rolling (CR), and at 375°C for 10 h after 90% cold-rolling or ARB process, and for the Cu-Ni-P-Zr specimens, aged at 450°C for 1h after 50% cold-rolling, and at 350°C for 30min after 90% cold-rolling or ARB process.

Specimen	Processing method	d (μm)	$\sigma_{0.2}$ (MPa)	σ_u (MPa)	ε_t (%)	σ (%IACS)
Cu-Ni-Be-Zr	50% CR + AG	28	660	700	10	59
	90%CR + AG	5	740	790	7	63
	ARB + AG	0.4	780	810	9	62

Specimen	Processing method	d (μm)	$\sigma_{0.2}$ (MPa)	σ_u (MPa)	ε_t (%)	σ (%IACS)
Cu-Ni-P-Zr	50% CR + AG	23	480	540	11	45
	90% CR + AG	4	590	630	6	42
	ARB + AG	0.4	600	640	8	42

Table 2 Grain size d, 0.2% proof stress $\sigma_{0.2}$, tensile strength σ_u, elongation ε_t and electrical conductivity σ for the Cu-Ni-P-Zr specimens, peak-aged (AG) at 400°C for 1h after pre-aging (AG) at 450°C for 5min and subsequent 50% rolling (CR), and at 400°C for 30min after pre-aging at 450°C for 5 min and subsequent 90%-rolling or ARB-process.

Processing method	d (μm)	$\sigma_{0.2}$ (MPa)	σ_u (MPa)	ε_t (%)	σ (%IACS)
AG + 50% CR + AG	21	570	610	8	50
AG + 90% CR + AG	3	730	770	4	56
AG + ARB + AG	0.3	740	780	6	56

recalled that the hardness for the 90%-RS and ARB-PS reached a maximum on aging at 350ºC for 30min, on which recrystallization began occurring. Therefore, the amount of precipitates produced by aging at 350ºC for 30min will be insufficient and thus suppression of the recrystallization during aging will result in the increase in strength.

It is widely accepted that, during the annihilation and rearrangement of dislocations to form low-angle boundaries on annealing a deformed metallic material, densely-dispersed fine particles pin individual dislocations and thus inhibit the stage of the recovery. As a result, recrystallization may be suppressed [7]. Thus, the solution-treated Cu-Ni-P-Zr alloy was initially aged at 450ºC for 5min to form fine precipitates, and then 90%-rolled or ARB-processed, and again aged at 450 or 400ºC. The amount of precipitation hardening by aging at 450ºC for 5min is about one third of its maximum amount. The Vickers hardness for the specimen re-aged at 450ºC showed a peak just after the occurrence of recrystallization, whereas the specimen re-aged at 400ºC exhibited a peak of hardness at 30min prior to the beginning of recrystallization.

Table 2 lists the values of d, $\sigma_{0.2}$, σ_u, ε_t and σ for the Cu-Ni-P-Zr specimens, peak-aged at 400°C for 1 h or 30min after pre-aging at 450°C for 5min and subsequent 50% rolling or 90% rolling and ARB-process. Comparison with Table 2 reveals that pre-aging at 450°C for 5min enhances remarkably 0.2% proof stress, tensile strength and electrical conductivity for each specimen. On the other hand, the values of ε_t are slightly reduced. The Cu-Ni-P-Zr alloy, ARB-processed and then peak-aged at 400ºC after pre-aging, exhibits the value of σ_u=780MPa, far larger than σ_u=670MPa for the Cu-0.7%Ni-0.13%P-0.1%Fe alloy, recently developed [6], although the values of ε_t=6% and σ=56%IACS for the present alloy are small compared with the values of ε_t=7% and σ=65%IACS for the commercial alloy.

TEM observations of the solution-treated alloys revealed that there existed no precipitates. Aging the Cu-Ni-Be-Zr alloy at 450ºC for 2 h after 50% rolling, and at 375ºC for 10 h after 90% rolling and ARB process produced disk-shaped γ" parallel to $\{100\}_\alpha$ of the Cu matrix [1]. Also, spherical $Ni_{12}P_5$ precipitates [2] were observed in the Cu-Ni-P-Zr alloy, peak-aged at 400°C for 1 h or 30min after pre-aging at 450°C for 5min and subsequent 50% rolling or 90% rolling and ARB-process. Figure 2 is an example of the disk-shaped γ" precipitates parallel to $(001)_\alpha$ in the Cu-Ni-Be-Zr specimen aged at 450^{o}C for 2 h after 50% rolling. In the aged Cu-Ni-Be-Zr and Cu-Ni-P-Zr specimens, no other precipitates existed, indicating that 0.1%Zr atoms dissolve in the Cu matrix even after aging.

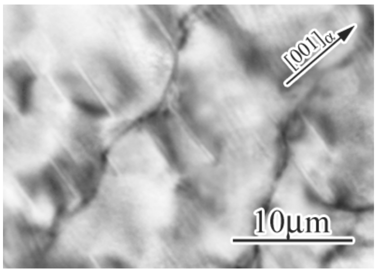

Fig. 2 TEM image of γ" precipitates in the Cu-Ni-Be-Zr specimen aged at 450^{o}C for 2 h after 50% cold-rolling.

4. Discussion

Ota *et al.* have reported that the yield stress of Cu-Ni-Be alloys containing γ" precipitates at room temperature is controlled by the Orowan mechanism at peak-age and over-age conditions [1]. The Orowan stress is inversely proportional to the inter-precipitate spacing λ. Nie and Muddle considered the statistical evaluation of the average spacing λ_{ave} between plate tips assuming that the precipitates form as circular disks and arrived at the following expression [8]

$$\lambda_{ave} = \sqrt{\frac{\sqrt{3}}{2}\frac{1}{\sqrt{2\sin\theta \cdot N \cdot r}}} - \frac{\pi r}{4} - \frac{\sqrt{3}}{2}\frac{h}{\sin\theta}. \quad (1)$$

Here N is the number density of precipitates per unit volume, r is the radius of disk-shaped precipitates, h is their thickness and θ is the dihedral angle between the plate and the $\{111\}_\alpha$ slip plane. For $\{001\}_\alpha$ precipitate plates, θ=54.74°. The radius and thickness of γ" precipitates were measured from high-resolution TEM images. The volume fraction f for the Cu-Ni-Be-Zr alloy was determined by applying the values of electrical resistivity, before and after aging, to the experimental data regarding the dependence of electrical resistivity on Ni or Be concentration [9]. The number density N of γ" precipitates was obtained from r, h and f using the equation of $N=f/(\pi r^2 h)$. Table 4 lists the values of r, h, f, N and λ_{ave}, together with $\sigma_{0.2}$, d and dislocation density ρ for the Cu-Ni-Be-Zr specimens, peak-aged at 450°C for 2 h or 375°C for 10 h after 50% rolling or 90% rolling and ARB process. The value of $\sigma_{0.2}$ for the 90%-RS is larger than that of the 50%-RS. This arises because of the smaller values of λ and d and the larger value of ρ for the 90%-RS. The ARB-PS exhibits the larger value of $\sigma_{0.2}$ than the 90%-RS. Since the values of λ and ρ for the ARB-PS and 90%-RS are nearly identical, the effect of grain refinement on the strength is reflected. From the grain size dependence of the yield stress, previously reported by Gertsman *et al.* [10], the increment in yield stress by the grain refinement from 5μm to 0.4μm can be estimated as about 60MPa, which is close to the difference between the values of $\sigma_{0.2}$ for the ARB-PS and 90%-RS.

Table 4 0.2% proof stress $\sigma_{0.2}$, volume fraction *f* of γ" precipitates, precipitate radius *r*, precipitate thickness *h*, precipitate number density *N*, inter-precipitate spacing λ, dislocation density ρ, and grain size *d* for the Cu-Ni-Be-Zr specimens, peak-aged (AG) at 450°C for 2h after 50% rolling (CR), and at 375°C for 10h after 90% rolling or ARB process.

Processing method	$\sigma_{0.2}$ (MPa)	f	r (nm)	h (nm)	N ($\times 10^{23}$/m^{-3})	λ (nm)	ρ ($\times 10^{14}$/m^{-2})	d (μm)
50% CR + AG	660	0.016	3.4	0.6	7.2	11	3.0±0.2	28
90% CR + AG	740	0.017	3.0	0.5	11	9.0	7.2±0.2	5
ARB + AG	780	0.017	2.7	0.5	15	8.9	7.0±0.3	0.4

Nomura *et al.* [2] have revealed that the yield stress at room temperature of a Cu-Ni-P system alloy containing spherical $Ni_{12}P_5$ precipitates is controlled by the Orowan mechanism at the peak-age or over-age condition. In this case, the inter-precipitate spacing λ is written as [3]

$$\lambda = \left[(2\pi/3f)^{1/2} - 1.63\right] \tag{2}$$

where r_s is the average radius of spherical precipitates. Table 5 shows the values of r_s, f, N and λ together with $\sigma_{0.2}$, d and ρ for the Cu-Ni-P-Zr specimens, peak-aged at 400°C for 1h or 30min after pre-aging at 450°C for 5min and subsequent 50% or 90% rolling and ARB process. The value of $\sigma_{0.2}$ for the 90%-RS is larger than that of the 50%-RS. On the other hand, different from the result shown in Table 4, the ARB-PS exhibits nearly the same value of $\sigma_{0.2}$ as the 90%-RS, regardless of the smaller value of d for the ARB- PS. The values of λ for the ARB-PS and 90%-RS are almost identical, whereas the value of ρ for the ARB-PS is smaller. Using the values of ρ for the ARB-PS and 90%-RS, the yield strength for the ARB-PS can be estimated to be low by about 60MPa from the Bailey-Hirsch relationship [11]

$$\Delta\sigma_d = M\alpha\mu b\sqrt{\rho}\ . \tag{3}$$

Here $\Delta\sigma_d$ is the increment in yield stress, M is the Taylor factor, α is a constant, μ is the shear modulus and b is the burgers vector. The values of M=3.06, α=0.57, μ=46GPa and b=0.256nm [12] were used. On the other hand, from the grain size dependence of the yield stress, previously reported by Gertsman *et al.* [10], the increment in yield stress by the grain refinement from 3μm to 0.3μm can be estimated as about 60MPa, which is comparable to about 40MPa from the Bailey-Hirsch relationship. Therefore, the reason why there is little difference in yield stress between the ARB-PS and 90%-RS can be understood.

Table 5 0.2% proof stress $\sigma_{0.2}$, volume fraction *f* of $Ni_{12}P_5$ precipitates, precipitate radius *r*, precipitate number density *N*, inter-precipitate spacing λ, dislocation density ρ, and grain size *d* for the Cu-Ni-P-Zr specimens, peak-aged (AG) at 400°C for 1h after pre-aging (AG) at 450°C for 5min and subsequent 50% rolling (CR), and at 400°C for 30min after pre-aging at 450°C for 5min and subsequent 90%-rolling or ARB-process.

Processing method	$\sigma_{0.2}$ (MPa)	f	r (nm)	N ($\times 10^{22}$/m^{-3})	λ (nm)	ρ ($\times 10^{14}$/m^{-2})	d (μm)
AG + 50% CR + AG	570	0.011	5.4	2.1	64	1.9±0.4	21
AG + 90% CR + AG	730	0.012	3.8	3.7	46	6.1±0.2	3
AG + ARB + AG	740	0.012	4.0	3.6	45	4.8±0.2	0.3

5. Conclusions

(1) The grain sizes of the Cu-1.2wt%Ni-0.2wt%Be-0.1wt%Zr and Cu-1.4wt%Ni-0.25wt%P-0.1wt%Zr alloys, severely deformed by 5-cycle ARB process or cold rolling to a 90% reduction, are nearly identical and refined down to about 0.4μm or 4μm.
(2) The Cu-Ni-Be-Zr alloy, ARB-processed and peak-aged at 375°C, has a tensile strength σ_u of 810MPa, an elongation ε_t of 9% up to failure and an electrical conductivity σ of 62%IACS. The Cu-Ni-P-Zr alloy, initially aged at 450°C, then ARB-processed and peak-aged at 400°C, exhibits the values of σ_u=780MPa, ε_t=6% and σ=56%IACS.

Acknowledgement

D. T. and N. T. of the authors appreciate the financial support by the Grant-in-Aid for Scientific Research on Innovative Area, "Bulk Nanostructured Metals", through MEXT, Japan (contract No. 22102002).

References

[1] Ota S, Muramatsu N, Watanabe C, Monzen R, *J Soc Mater Sci Japan* 2007; **56(6)**: 531-536.
[2] Nomura K, Miwa Y, Shimada Y, Watanabe C, Monzen R, *J Japan Inst Metals* 2010; **74(5)**: 325-330.
[3] Watanabe C, Hiraide H, Zhang Z, Monzen R, *J Soc Mater Sci Japan* 2005; **54(7)**: 717-723.
[4] Saito Y, Tsuji N, Utsunomiya H, Sakai T, Hong H.G, *Scripta Mater* 1998; **39**: 1221-1227.
[5] Kunieda T, Nakai M, Murata Y, Koyama T, Morinaga M, *ISIJ International* 2005; **45**: 1909-1914.
[6] Ozaki R, Miwa Y, *R&D Kobe Steel Engineering Reports* 2007; **57**: 110.
[7] Kita K, Kobayashi K, Monzen R, *J Soc Mater Sci Japan* 2000; **49**: 482.
[8] Nie JF, Muddle BC, Polmear IJ, *Mater Sci Forum* 1996; **217**: 1257-1262.
[9] Komatsu S, *J JRICu* 2002; **41**: 1-9.
[10] Gertsman V.Y, Hoffmann M, Gleiter H, Birringer R, *Acta Metall Mater* 1994; **42**: 3539-3544.
[11] Bailey J.E, Hirsch P.B, *Philos Mag* 1960; **5**: 485-497.
[12] Staker M.R, Holt D.L, *Acta Metall* 1972; **20**: 569-579.